SUPPLEMENTAL MATERIAL

Supplementary Methods

Figure S1. The missingness of all the echo variables.

Figure S2. Identification of novel clinical subtypes with ConsensusClusterPlus.

Figure S3. Comparisons of the two subtypes after dividing patients into 6 groups by age at enrollment.

Figure S4. Estimated survival curves for primary endpoints at means of all other covariates.

Figure S5. Multidimensional scaling (MDS) analysis of genetic race using data from the 1000 Genomes Project as anchors.

Figure S6. Comparison of proportions of specific gene carriers between two subtypes.

Figure S7. Comparison of likelihood of experiencing cardiac death between HCM associated gene carriers and non-carriers.

Figure S8. Performance of HCM associated genes in predicting subtype propensity and disease prognosis (cardiac death).

Figure S9. The optimal C value searching process in logistic regression model with L1 penalty term.

Figure S10. Correlation analysis for predicted score and representative echocardiography variables.

Figure S11. Effect of increasing probability for subtype 1 on predicted risk of experiencing cardiac death and progression to NYHA class III/IV.

Figure S12. PPI network analysis.

Figure S13. Samples of second population were divided into quartiles based on probability for subtype 1.

Figure S14. The performance of 46-gene model and integrated model in the first cohort (training set) and second cohort (testing set).

Figure S15. The performance of models based on different MAF threshold for rare variants.

Table S1. Quality control report for WES.

Table S2. Genes associated with HCM.

Table S3. Characteristics of subtypes after propensity score matching.

Table S4. Univariate Cox regression analysis for cardiovascular death during follow-up.

Table S5. Multivariable Cox regression analysis for cardiovascular death during follow-up.

Table S6. Multivariable Cox regression analysis for progression to NYHA Class III-IV during follow-up.

Table S7. Putative causal mutations in HCM-associated genes identified in our cohort.

Table S8. Comprehensive annotation for identified genes.

Table S9. Clinical status of heart tissue from published database.

Table S10. 46-gene set was enriched in LVEF-reduced HCM patients after adjusting for multiple comparisons.

Supplemental Methods

DNA preparation

DNA was isolated from each peripheral blood sample using the QIAamp DNA blood Mini Kit (Qiagen), according to the manufacturer's instructions. DNA quality and quantity were analyzed with a NanoDrop (ThermoFisher) and agarose gel electrophoresis (AGE). The qualified genomic DNA samples were subjected to subsequent whole exome sequencing.

Whole exome sequencing

DNA sample was randomly fragmented by Covaris technology and ligated with adapters, amplified, purified and hybridized to the exome array. Captured products were subjected to Agilent 2100 Bioanalyzer and quantitative PCR to estimate the magnitude of enrichment. Each qualified captured library was then loaded on Illumina platforms, and high-throughput sequencing was performed for each captured library. Then we followed the Genome Analysis Toolkit (GATK) Best Practices workflow for the whole exome sequencing analysis.[1] Briefly, valid raw data was mapped to hg19 human reference genome using Burrows-Wheeler Aligner (BWA) software.[2] After sorting BAM file and marking duplication, Indel realignment and base quality recalibration were carried out by GATK, with duplicate reads removed by Picard tools. The final BAM files were then used for variant calling and variant quality score recalibration (VQSR). The HaplotypeCaller of GATK was used to call both SNPs and InDels simultaneously via local de-novo assembly of haplotypes. Subsequent VQSR was performed with following parameters: QualByDepth, FisherStrand, RMSMappingQuality, MappingQualityRankSumTest, ReadPosRankSum. Only variants tagged with "PASS" were subjected to downstream analysis. The principal component analysis (PCA) for population stratification was conducted to excluded batch effect with Eigenstrata, using the linkage disequilibrium-pruned common variants with a minor allele frequency (MAF) of >0.05.[3] High-confident variants were then annotated using ANNOVAR.[4]

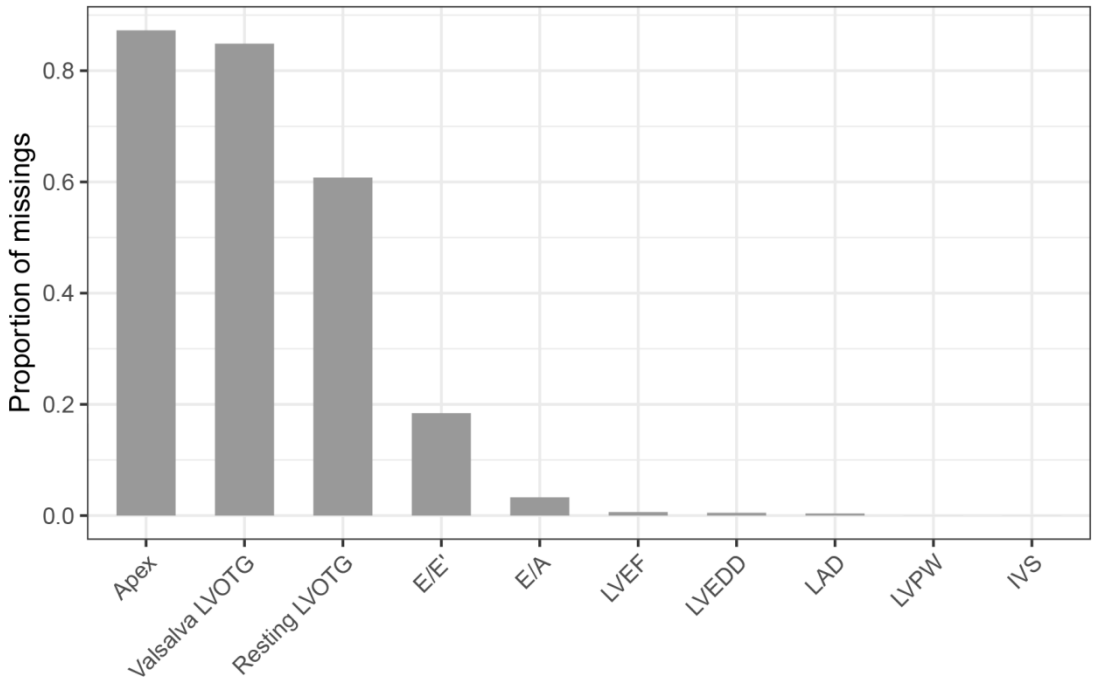

Figure S1. The missingness of all the echo variables. Any missing data were handled by omission from the respective analyses.

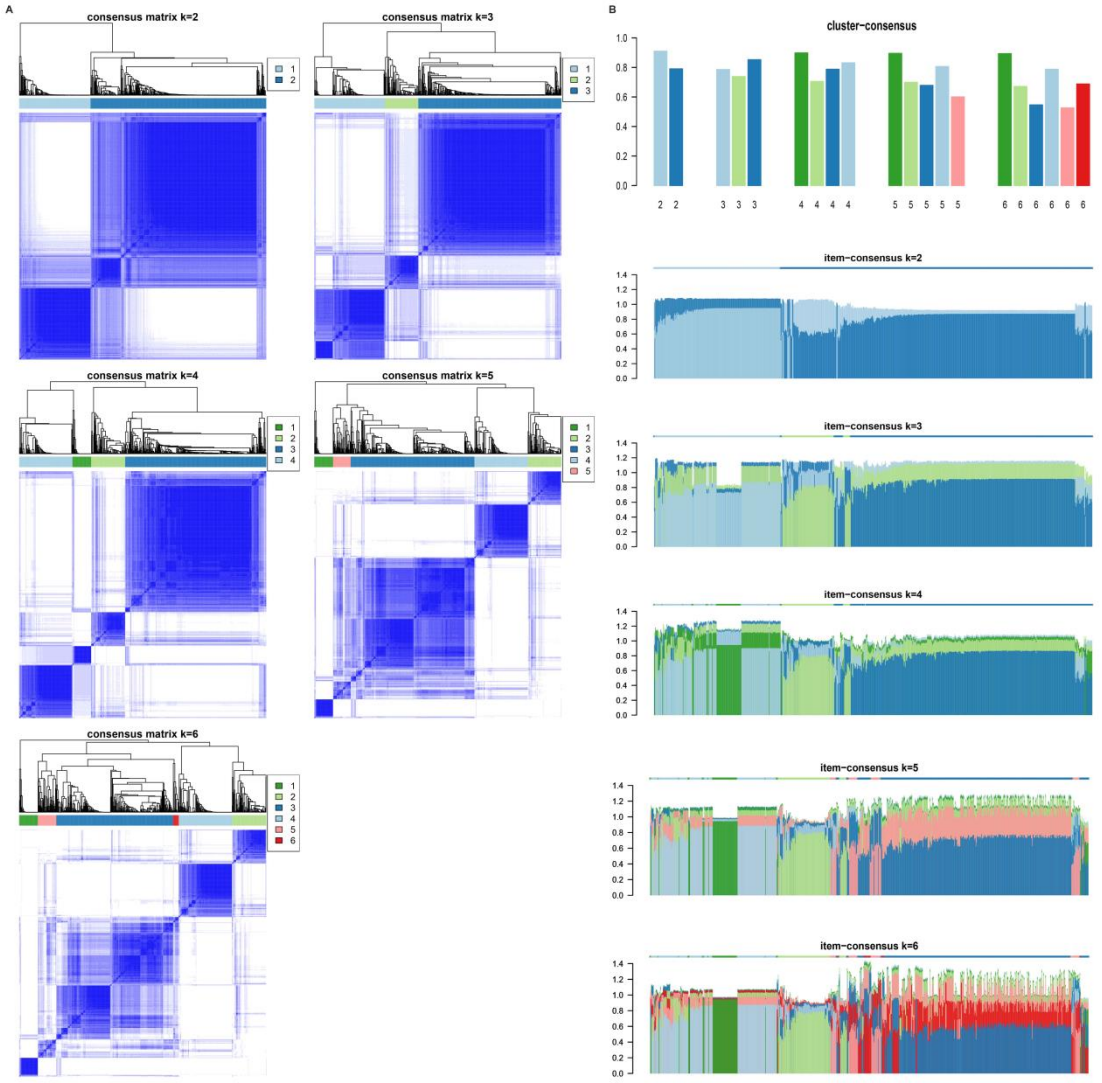

Figure S2. Identification of novel clinical subtypes with ConsensusClusterPlus.

(A) Consensus matrix for k =2 to 6. (B) Cluster-consensus plot and item-consensus plot for k = 2 to 6.

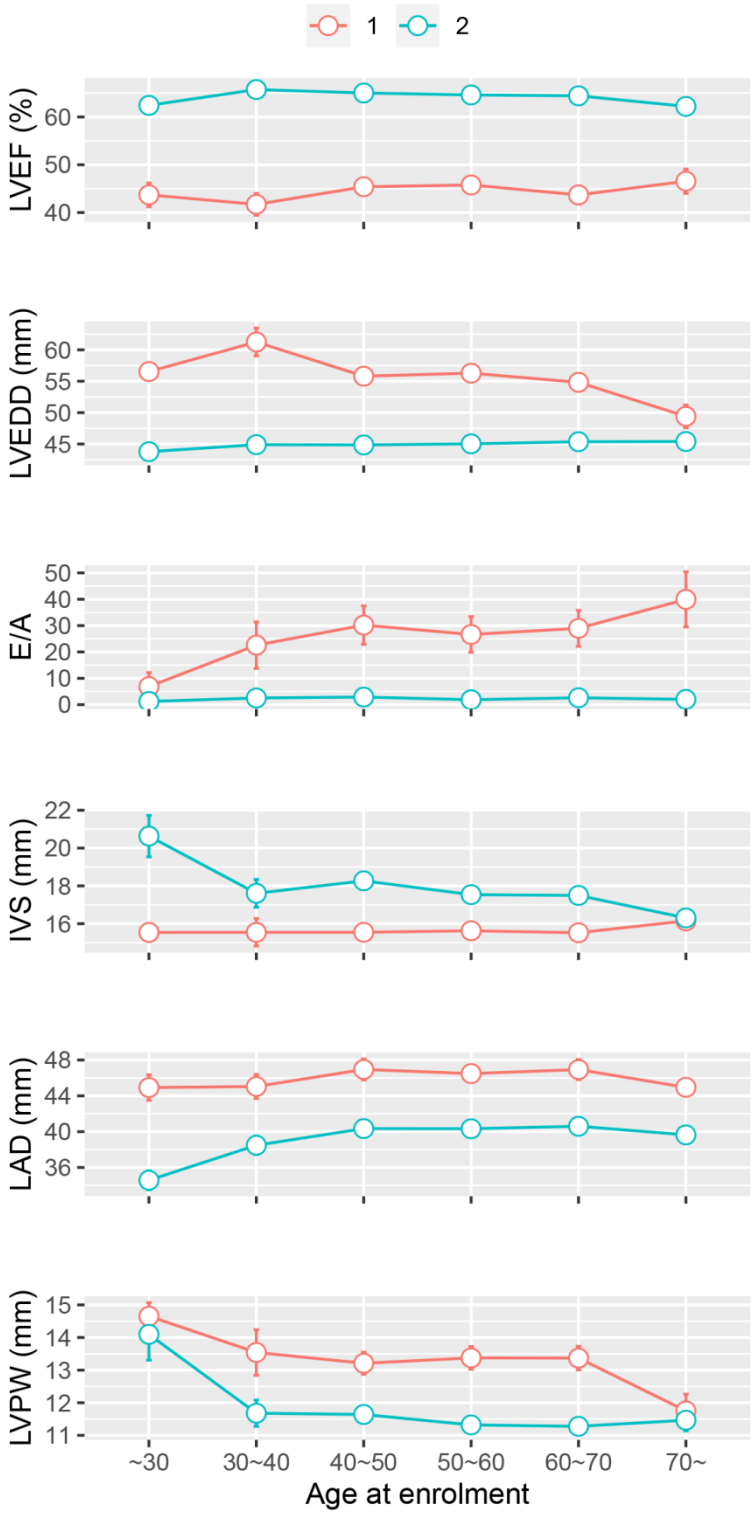

Figure S3. Comparisons of the two subtypes after dividing patients into 6 groups by age at enrollment.

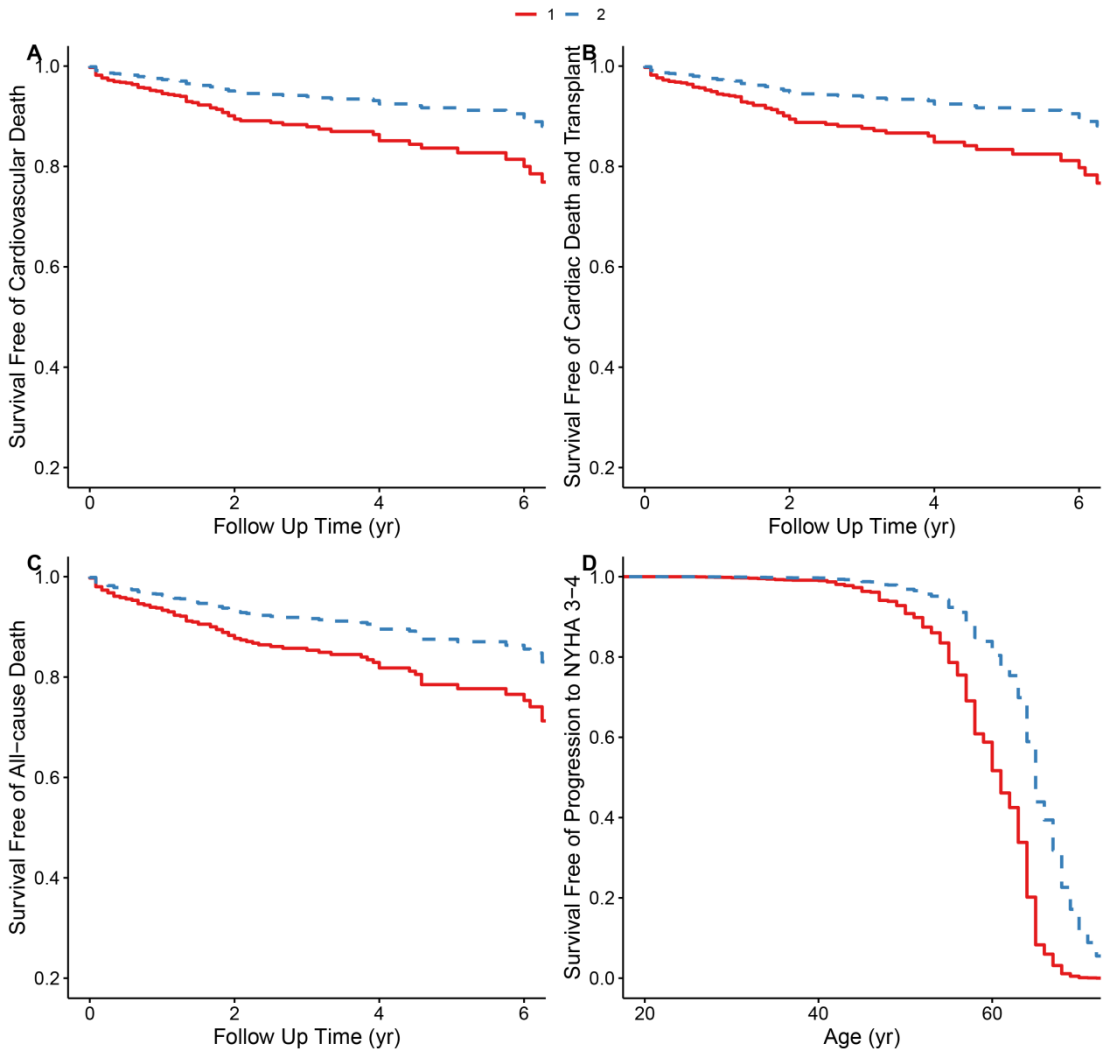

Figure S4. Estimated survival curves for primary endpoints at means of all other covariates.

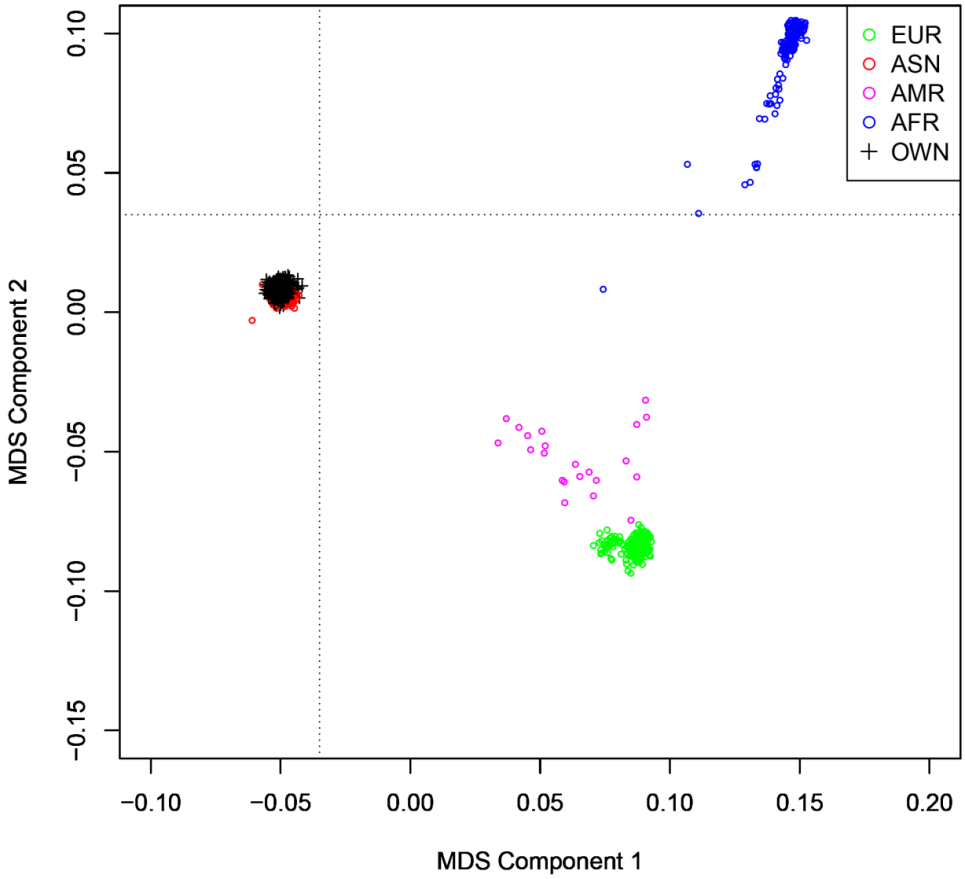

Figure S5. Multidimensional scaling (MDS) analysis of genetic race using data from the 1000 Genomes Project as anchors.

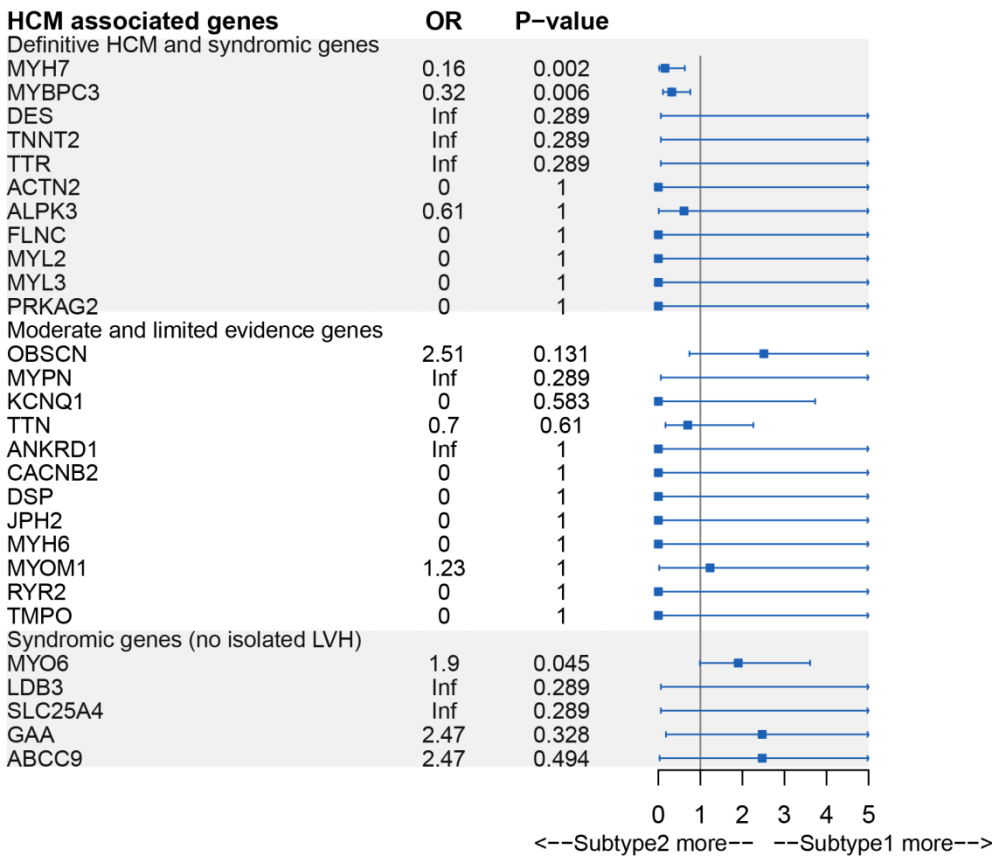

Figure S6. Comparison of proportions of specific gene carriers between two subtypes. OR >1 indicate a higher proportion in subtype 1.

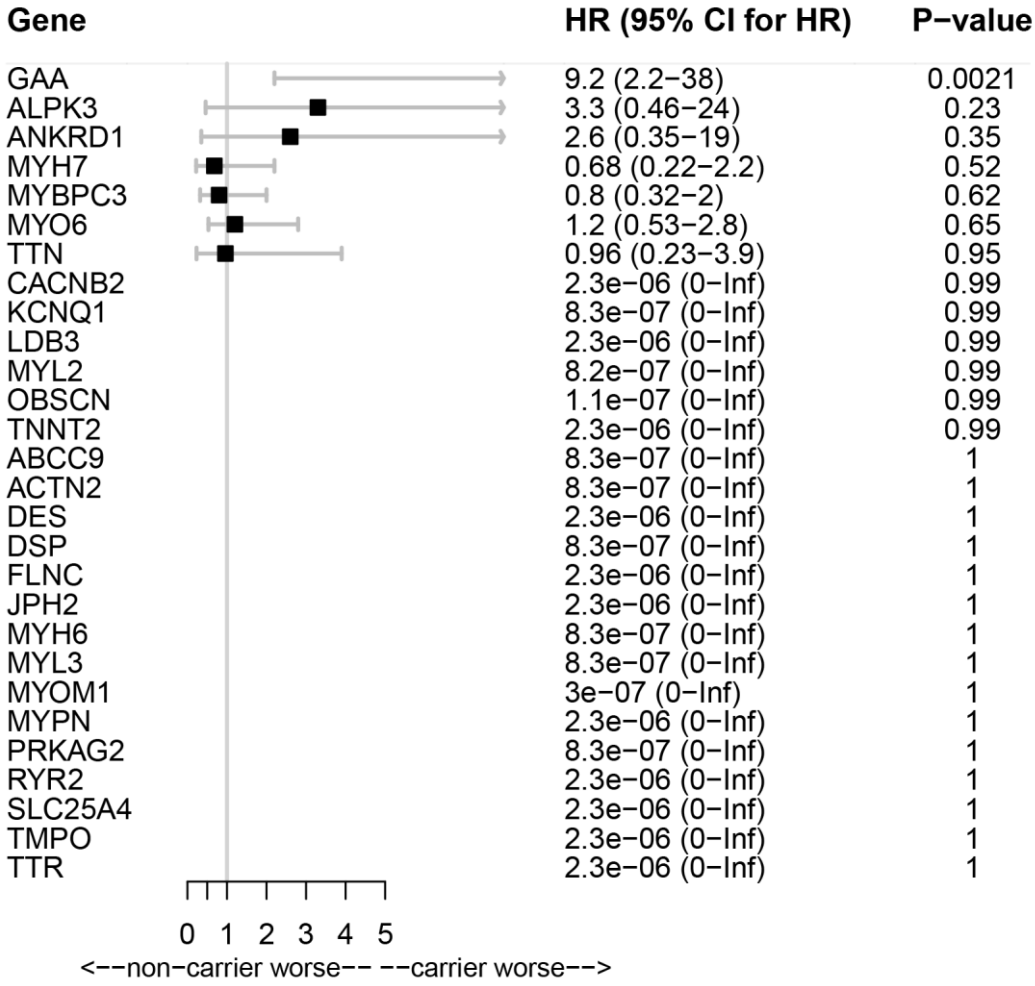

Figure S7. Comparison of likelihood of experiencing cardiac death between HCM associated gene carriers and non-carriers. Hazard Ratio was calculated with univariate Cox regression.

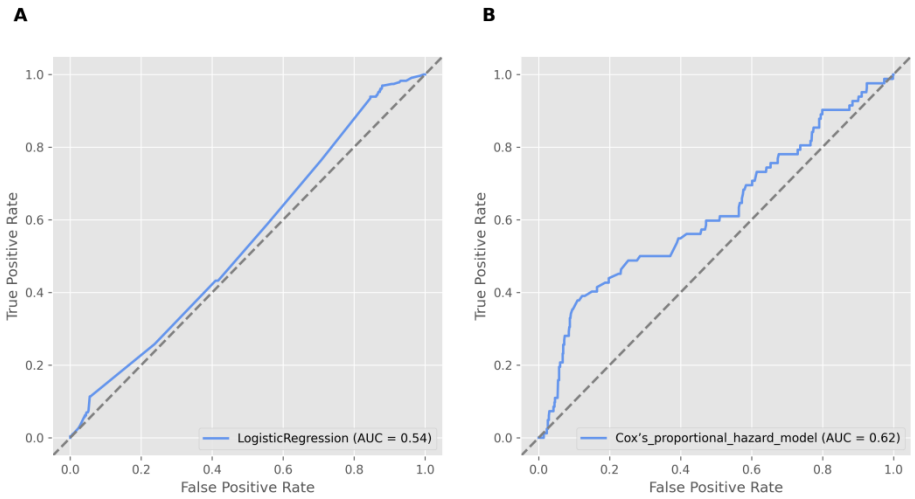

Figure S8. Performance of HCM associated genes in predicting subtype propensity and disease prognosis (cardiac death). (A) ROC curve for the prediction of subtype classification using mutations in HCM associated genes. **(B)** ROC curve for the prediction of disease prognosis (cardiac death) using mutations in HCM associated genes. AUC, area under the curve, was measured by stratified 5-fold cross validation.

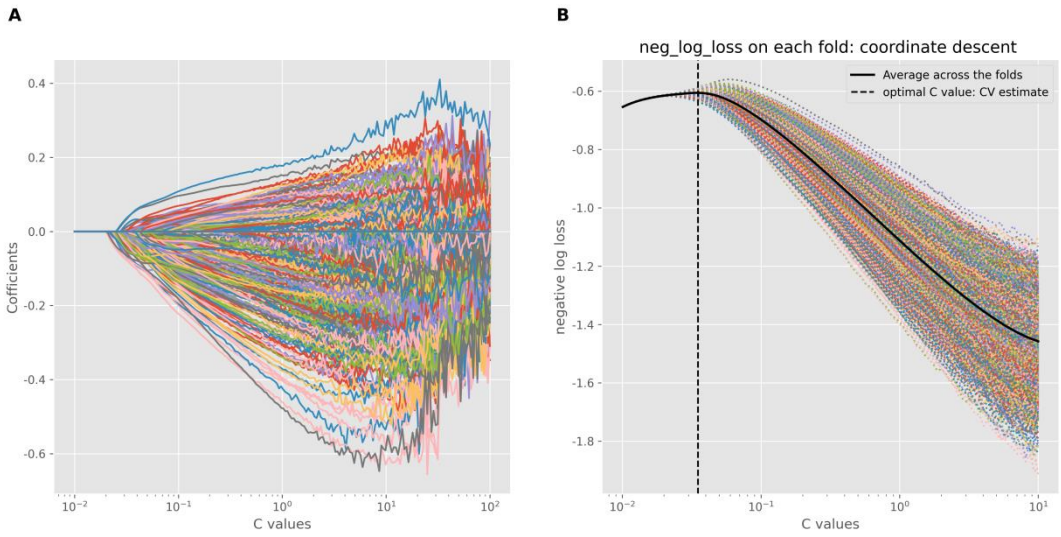

Figure S9. The optimal C value searching process in logistic regression model with L1 penalty term. (A) coefficient of each gene included in the model approached 0 with the decrease of *C* value and finally converged to 0. **(B)** The optimal *C* value was determined by 1000 times stratified 5-fold cross-validation.

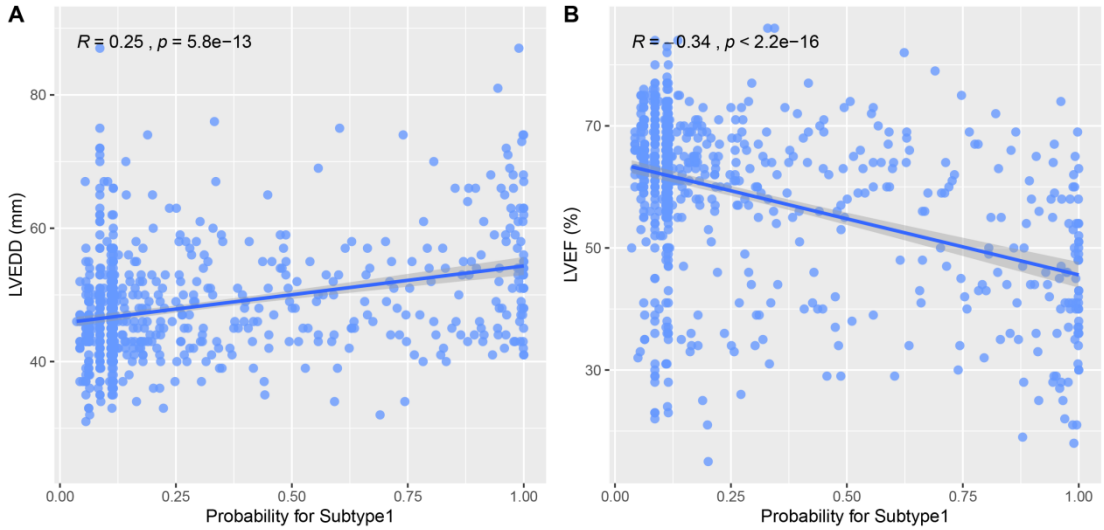

Figure S10. Correlation analysis for predicted score and representative echocardiography variables.

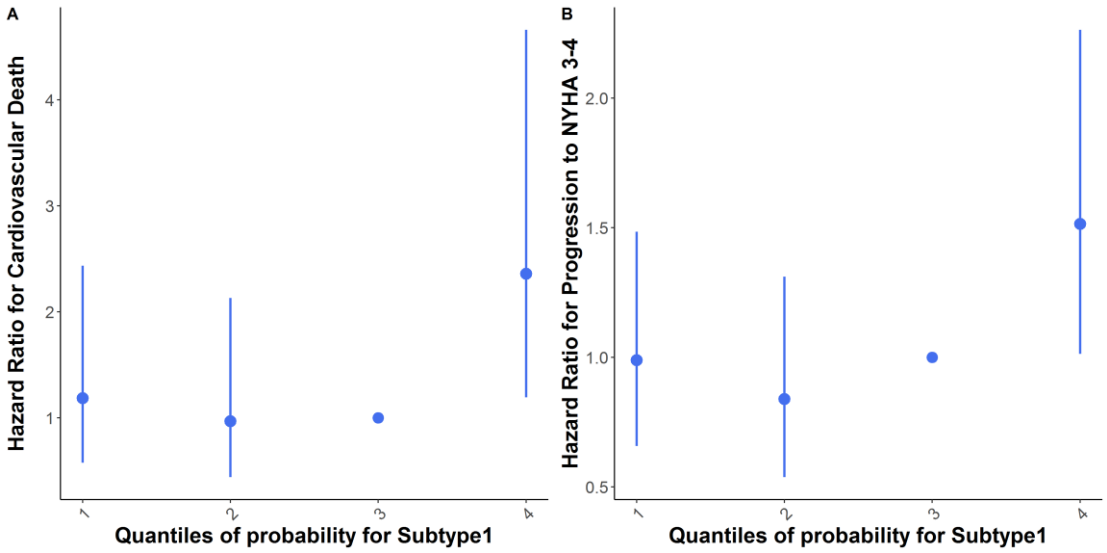

Figure S11. Effect of increasing probability for subtype 1 on risk of experiencing cardiac death and progression to NYHA class III/IV.

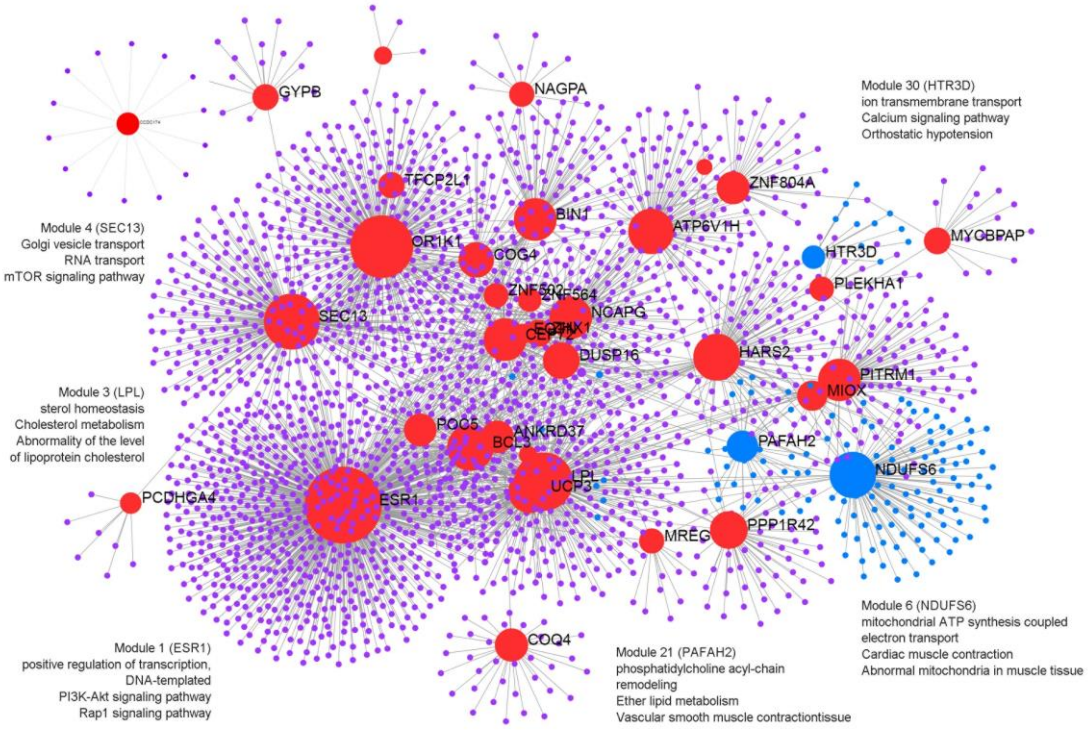

Figure S12. Network topology analysis. Modules identified by mapping feature genes onto PPI network adopting InfoMap algorithm. Modules displaying differential expression were colored in blue and labeled with the most representative biological processes and KEGG pathways.

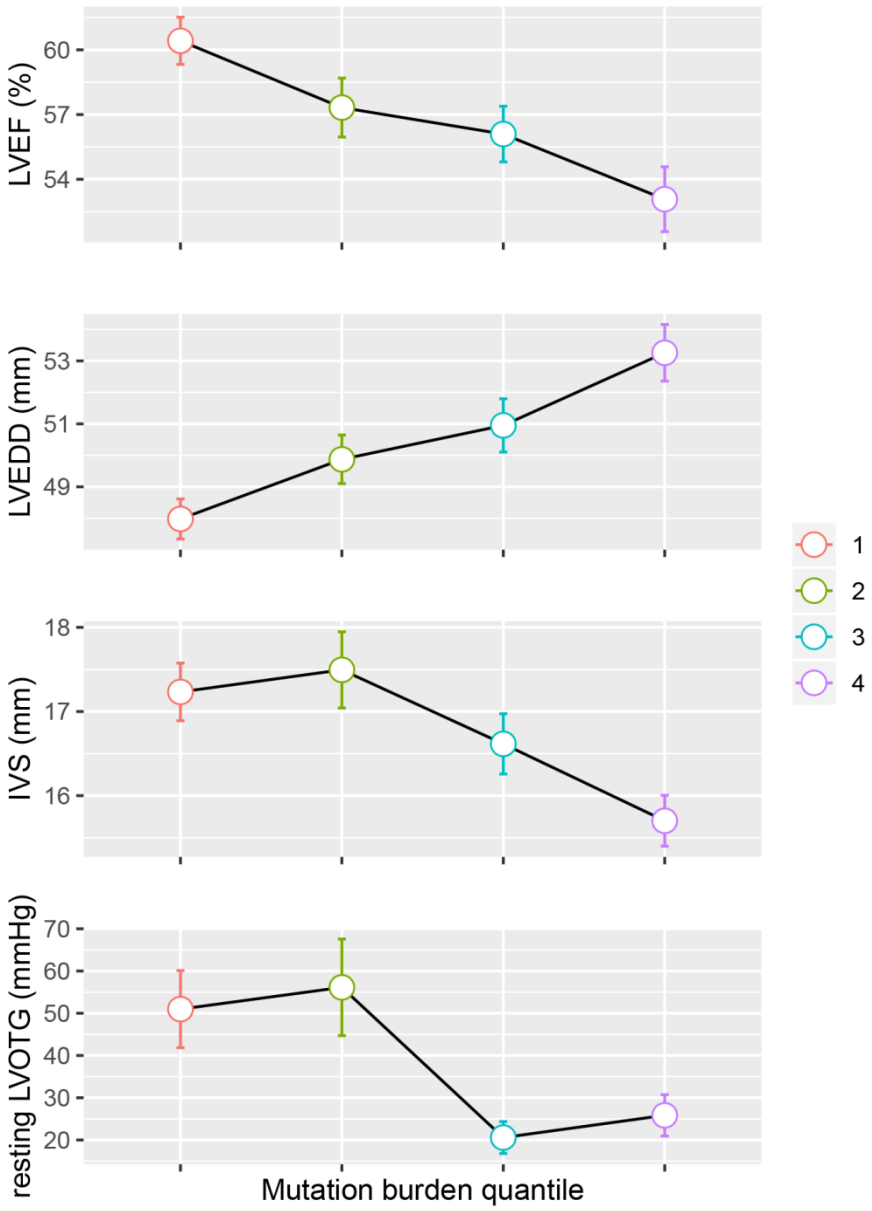

Figure S13. Samples of second population were divided into quartiles based on predicted probability for subtype 1 by 46-gene model.

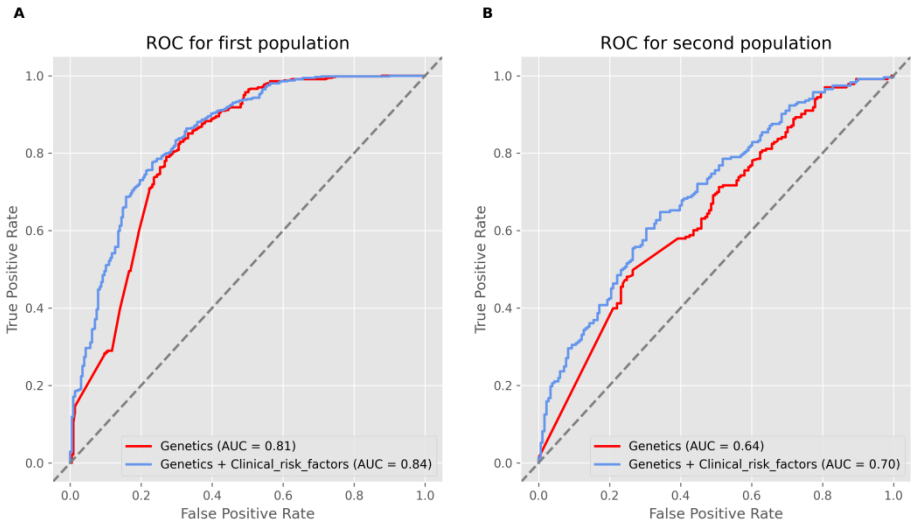

Figure S14. The performance of 46-gene model and integrated model in the first cohort (training set) and second cohort (testing set).

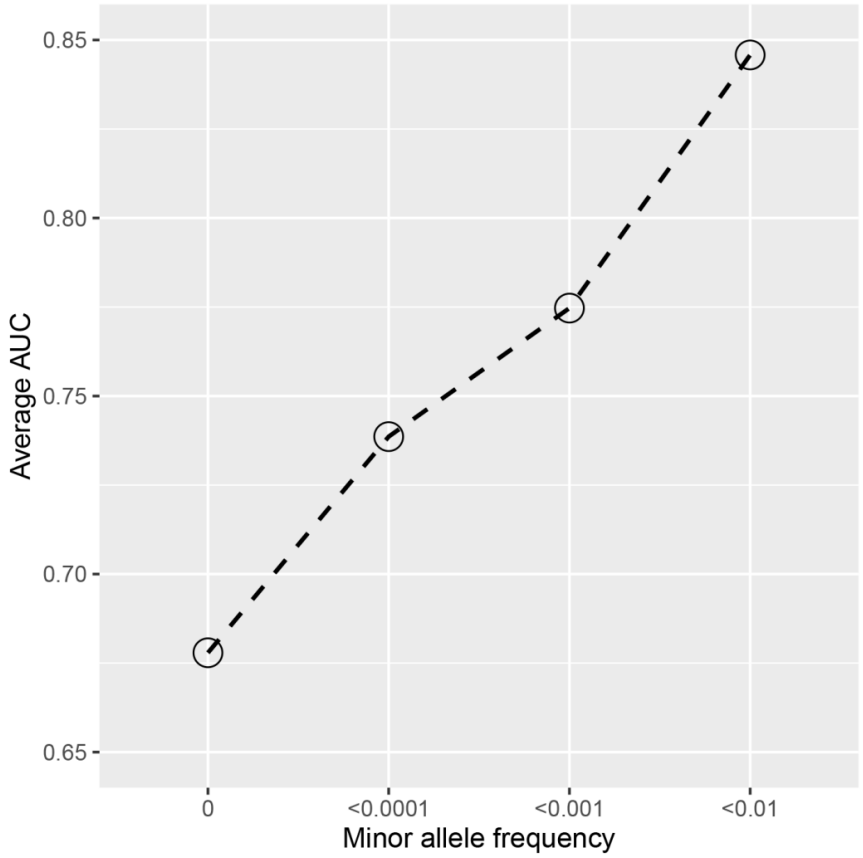

Figure S15. The performance of models based on different MAF threshold for rare variants. Average AUC showed that predictions were optimal only when we included variants with MAF < 0.01 in 1000 Genomes Project, Exome Aggregation Consortium and Genome Aggregation Database

Table S1. Quality control report for WES.

Average sequencing depth on target	99.65
Fraction of target covered >= 4x (%)	99.00
Fraction of target covered >= 10x (%)	98.26
Fraction of target covered >= 20x (%)	95.41

Table S2. Genes associated with HCM.

Definitive HCM and syndromic genes	Moderate and limited evidence genes	Syndromic genes (no isolated LVH)
MYL2	CSRP3	ABCC9
TNNT2	TNNC1	BAG3
ACTC1	JPH2	CAV3
MYBPC3	TTN	COX15
MYH7	KLF10	CRYAB
TPM1	MYPN	FXN
TNNI3	ANKRD1	GAA
MYL3	MYLK2	LDB3
PLN	MYOZ2	MYO6
CACNA1C	NEXN	SLC25A4
DES	VCL	
FHL1	TRIM63	
FLNC	RYR2	
GLA	MYH6	
LAMP2	OBSCN	
PRKAG2	PDLIM3	
PTPN11	TCAP	
RAF1	MYOM1	
RIT1	CALR3	
TTR	ACTA1	
	CASQ2	
	CACNB2	
	DSP	
	KCNQ1	
	TMPO	
	ACTN2	
	ALPK3	

Table S3. Characteristics of subtypes after propensity score matching.

	Subtype 1 n =183	Subtype 2 n =323	p value
Age of onset (yrs)	51.34 (13.96)	50.74 (13.86)	0.64
Age at enrolment (yrs)	51.96 (14.15)	52.17 (13.46)	0.87
Gender = male (%)	149 (81.4)	252 (78.0)	0.428
Smoke (%)	72 (39.3)	135 (41.8)	0.656
Drink (%)	50 (27.3)	100 (31.0)	0.448
CAD (%)	48 (26.2)	78 (24.1)	0.68
Diabetes (%)	38 (20.8)	61 (18.9)	0.692
Systolic blood pressure (mmHg)	127.88 (18.14)	127.46 (14.62)	0.777
Diastolic blood pressure (mmHg)	77.57 (11.64)	76.99 (10.06)	0.557
IVS (mm)	15.62 (2.50)	17.89 (4.75)	<0.001
LVPW (mm)	13.36 (2.62)	11.77 (3.14)	<0.001
Apex (mm)	16.67 (4.46)	17.86 (3.51)	0.439
LAD (mm)	46.14 (6.49)	39.51 (7.28)	<0.001
LVEDD (mm)	55.54 (9.60)	45.26 (5.15)	<0.001
LVEF (%)	44.99 (12.60)	64.20 (8.20)	<0.001
Resting LVOTG (mmHg)	30.41 (43.94)	40.34 (51.16)	0.377
Valsalva LVOTG (mmHg)	32.88 (24.77)	51.58 (44.78)	0.253
E/A	28.11 (47.11)	2.48 (11.31)	<0.001
E/E'	22.54 (12.10)	16.64 (8.21)	<0.001

Table S4. Univariate Cox regression analysis for cardiovascular death during follow-up.

		95.0% CI for H.R.		
Variables	H.R.	Lower	Upper	Sig.
Subtype =1	2.68	1.73	4.14	9.71e-06
Age at enrolment	1.03	1.02	1.05	0.0001
Gender = male	0.65	0.42	1.02	0.0607
NYHA Class III–IV	3.22	2.08	4.98	1.49e-07
Smoke	1.11	0.71	1.73	0.65
Drink	0.90	0.54	1.51	0.69
Diabetes	0.88	0.49	1.58	0.67
CAD	0.76	0.44	1.31	0.32
Atrial fibrillation	2.54	1.54	4.17	0.0002

Table S5. Multivariable Cox regression analysis for cardiovascular death during follow-up.

		95.0% CI for H.R.		
Covariates	H.R.	Lower	Upper	Sig.
Subtype =1	2.24	1.36	3.68	0.0015
Age at enrolment	1.03	1.01	1.04	0.0036
Gender = male	0.62	0.39	1.00	0.0524
NYHA Class III–IV	2.11	1.31	3.38	0.002
Atrial fibrillation	1.44	0.85	2.45	0.1714

Table S6. Multivariable Cox regression analysis for progression to NYHA Class III-IV during follow-up.

		95.0% CI for H.R.		
Covariates	H.R.	Lower	Upper	Sig.
Subtype =1	1.48	1.01	2.18	0.0468
Gender = male	0.88	0.66	1.18	0.3895
LVEF (per %)	0.97	0.96	0.98	2.02e-06

Table S7. Putative causal mutations in HCM-associated genes identified in our cohort.

Chromosome	Position	Translational effect	Gene symbol	Amino acid change	MAF in 1,000 Genomes (EAS)	MAF in ExAC (EAS)	MAF in gnomAD exome (EAS)	Pathogenicity determined by ACMG
chr12	111352091	missense	MYL2	p.R58Q	ND	0	0	Likely pathogenic
chr1	201334426	missense	TNNT2	p.R87W	ND	0	0	Likely pathogenic
chr11	47353660	frameshift deletion	MYBPC3	p.Q1259fs	ND	ND	ND	Likely pathogenic
chr11	47354119	frameshift deletion	MYBPC3	p.P1208fs	ND	ND	0	Likely pathogenic
chr11	47354220	frameshift insertion	MYBPC3	p.L1175fs	ND	ND	ND	Likely pathogenic
chr11	47354777	frameshift insertion	MYBPC3	p.Y1100fs	ND	ND	0	Likely pathogenic
chr11	47354782	stopgain	MYBPC3	p.W1098X	ND	ND	ND	Pathogenic
chr11	47355233	frameshift insertion	MYBPC3	p.R1022fs	ND	ND	ND	Likely pathogenic
chr11	47355246	frameshift deletion	MYBPC3	p.E1010fs	ND	ND	ND	Likely pathogenic
chr11	47355248	frameshift insertion	MYBPC3	p.E1017fs	ND	ND	ND	Likely pathogenic
chr11	47355264	frameshift deletion	MYBPC3	p.G1011fs	ND	ND	ND	Likely pathogenic
chr11	47356682	frameshift insertion	MYBPC3	p.R939fs	ND	ND	ND	Likely pathogenic
chr11	47356752	frameshift insertion	MYBPC3	p.W916fs	ND	ND	ND	Likely pathogenic

chr11	47356760	splicing	MYBPC3		ND	ND	ND	Likely pathogenic
chr11	47357496	stopgain	MYBPC3	p.W890X	ND	ND	ND	Pathogenic
chr11	47359010	missense	MYBPC3	p.R845H	ND	0	1.00E-04	Likely pathogenic
chr11	47359025	frameshift deletion	MYBPC3	p.R834fs	ND	ND	ND	Likely pathogenic
chr11	47359346	splicing	MYBPC3		ND	ND	ND	Likely pathogenic
chr11	47360071	missense	MYBPC3	p.D770N	ND	0	0	Pathogenic
chr11	47360090	frameshift deletion	MYBPC3	p.N763fs	ND	ND	ND	Likely pathogenic
chr11	47360225	frameshift insertion	MYBPC3	p.L718fs	ND	ND	ND	Likely pathogenic
chr11	47361219	stopgain	MYBPC3	p.Q684X	ND	ND	ND	Pathogenic
chr11	47362731	stopgain	MYBPC3	p.E619X	ND	ND	ND	Pathogenic
chr11	47363607	frameshift deletion	MYBPC3	p.G575fs	ND	ND	ND	Likely pathogenic
chr11	47364249	missense	MYBPC3	p.R502W	ND	0	0	Pathogenic
chr11	47364460	frameshift deletion	MYBPC3	p.P459fs	ND	ND	ND	Likely pathogenic
chr11	47364620	stopgain	MYBPC3	p.Q435X	ND	ND	ND	Pathogenic
chr11	47365079	stopgain	MYBPC3	p.W396X	ND	ND	ND	Pathogenic
chr11	47369407	splicing	MYBPC3		ND	0	8.54E-05	Likely pathogenic
chr11	47369413	frameshift deletion	MYBPC3	p.R272fs	ND	ND	ND	Likely pathogenic
chr11	47369975	missense	MYBPC3	p.E258K	ND	0	0	Pathogenic
chr11	47371563	splicing	MYBPC3		ND	ND	ND	Likely pathogenic
chr11	47372789	splicing	MYBPC3		ND	ND	0	Likely pathogenic

chr14	23883310	missense	MYH7	p.T1854M	ND	0	0	Likely pathogenic
chr14	23887498	missense	MYH7	p.A1364T	ND	0.0006	5.00E-04	Likely pathogenic
chr14	23888715	missense	MYH7	p.R1277Q	ND	0.0001	5.80E-05	Likely pathogenic
chr14	23891399	missense	MYH7	p.R1079W	0.002	0.0007	5.00E-04	Likely pathogenic
chr14	23891500	missense	MYH7	p.R1045H	ND	0	2.00E-04	Likely pathogenic
chr14	23893145	missense	MYH7	p.E965K	ND	ND	ND	Likely pathogenic
chr14	23893268	missense	MYH7	p.E924K	ND	ND	ND	Likely pathogenic
chr14	23894048	missense	MYH7	p.R870H	ND	0	0	Pathogenic
chr14	23894084	missense	MYH7	p.R858H	ND	0	0	Likely pathogenic
chr14	23894178	missense	MYH7	p.W827R	ND	ND	ND	Likely pathogenic
chr14	23894189	missense	MYH7	p.G823E	ND	ND	ND	Likely pathogenic
chr14	23896042	missense	MYH7	p.R663H	ND	0	0	Pathogenic
chr14	23896866	missense	MYH7	p.V606M	ND	ND	ND	Likely pathogenic
chr14	23896932	missense	MYH7	p.G584S	ND	ND	ND	Likely pathogenic
chr14	23898214	missense	MYH7	p.R453C	ND	ND	ND	Likely pathogenic
chr14	23898247	missense	MYH7	p.R442C	0.001	0	0	Likely pathogenic
chr14	23898464	missense	MYH7	p.V411I	ND	0	5.80E-05	Likely pathogenic
chr14	23898488	missense	MYH7	p.R403W	ND	ND	ND	Likely pathogenic
chr14	23899059	missense	MYH7	p.A355T	ND	ND	ND	Likely pathogenic
chr14	23900677	missense	MYH7	p.R249Q	ND	ND	ND	Likely pathogenic
chr14	23901046	missense	MYH7	p.T188N	ND	ND	ND	Likely pathogenic
chr14	23901923	missense	MYH7	p.R143W	ND	0.0001	1.00E-04	Likely pathogenic
chr3	46899899	missense	MYL3	p.D178E	ND	ND	ND	Likely pathogenic
chr3	46900980	missense	MYL3	p.V156L	ND	ND	5.80E-05	Likely pathogenic
chr3	52486161	frameshift deletion	TNNC1	p.P54fs	ND	0.0001	5.80E-05	Likely pathogenic

chr20	42744882	frameshift insertion	JPH2	p.P478fs	ND	ND	ND	Likely pathogenic
chr2	179393947	splicing	TTN		ND	ND	ND	Likely pathogenic
chr2	179431835	frameshift deletion	TTN	p.V17276fs	ND	ND	ND	Likely pathogenic
chr2	179446880	frameshift insertion	TTN	p.M13007fs	ND	ND	ND	Likely pathogenic
chr2	179473331	splicing	TTN		ND	ND	ND	Likely pathogenic
chr2	179474298	splicing	TTN		ND	ND	ND	Likely pathogenic
chr2	179481716	frameshift deletion	TTN	p.S6901fs	ND	ND	ND	Likely pathogenic
chr2	179517660	splicing	TTN		ND	ND	3.00E-04	Likely pathogenic
chr2	179532364	splicing	TTN		ND	ND	ND	Likely pathogenic
chr2	179546102	splicing	TTN		ND	ND	5.82E-05	Likely pathogenic
chr2	179558417	splicing	TTN		ND	ND	ND	Likely pathogenic
chr2	179581821	splicing	TTN		ND	ND	ND	Likely pathogenic
chr2	179595487	frameshift deletion	TTN	p.K4680fs	ND	ND	ND	Likely pathogenic
chr2	179610796	frameshift insertion	TTN	p.C5444fs	ND	ND	ND	Likely pathogenic
chr2	179611009	stopgain	TTN	p.L5373X	ND	ND	ND	Pathogenic
chr2	179613873	stopgain	TTN	p.Y4418X	0.001	0.0007	9.00E-04	Pathogenic
chr2	179614061	stopgain	TTN	p.Q4356X	ND	ND	ND	Pathogenic
chr2	179614178	stopgain	TTN	p.Q4317X	ND	0.0001	1.00E-04	Pathogenic
chr2	179614555	frameshift deletion	TTN	p.T4191fs	ND	ND	ND	Likely pathogenic

chr2	179615321	stopgain	TTN	p.R3936X	ND	0	2.00E-04	Pathogenic
chr2	179620948	splicing	TTN		0.001	0.0001	1.00E-04	Likely pathogenic
chr2	179621414	stopgain	TTN	p.E3426X	ND	ND	ND	Pathogenic
chr2	179655434	splicing	TTN		0.001	0.0005	4.00E-04	Likely pathogenic
chr10	69902871	frameshift deletion	MYPN	p.G360fs	ND	ND	ND	Likely pathogenic
chr10	92675561	frameshift deletion	ANKRD1	p.A243fs	ND	ND	ND	Likely pathogenic
chr10	92679010	frameshift insertion	ANKRD1	p.L75fs	ND	0	6.01E-05	Likely pathogenic
chr1	237617721	frameshift insertion	RYR2	p.K441fs	ND	ND	ND	Likely pathogenic
chr1	237617723	frameshift insertion	RYR2	p.A442fs	ND	ND	ND	Likely pathogenic
chr1	237617731	frameshift deletion	RYR2	p.V445fs	ND	ND	ND	Likely pathogenic
chr1	237617737	frameshift insertion	RYR2	p.L447fs	ND	ND	ND	Likely pathogenic
chr1	237617739	frameshift deletion	RYR2	p.P448fs	ND	ND	ND	Likely pathogenic
chr1	237617754	frameshift insertion	RYR2	p.V452fs	ND	ND	ND	Likely pathogenic
chr1	237617757	frameshift insertion	RYR2	p.S453fs	ND	ND	ND	Likely pathogenic
chr14	23851265	frameshift insertion	MYH6	p.M1935fs	ND	0	0	Likely pathogenic

chr14	23857465	stopgain	MYH6	p.K1420X	ND	ND	ND	Pathogenic
chr1	228399998	frameshift deletion	OBSCN	p.R172fs	ND	ND	ND	Likely pathogenic
chr1	228400009	frameshift deletion	OBSCN	p.P176fs	ND	ND	ND	Likely pathogenic
chr1	228400279	frameshift deletion	OBSCN	p.K266fs	ND	ND	ND	Likely pathogenic
chr1	228400355	stopgain	OBSCN	p.Q291X	ND	ND	ND	Pathogenic
chr1	228437942	splicing	OBSCN		ND	ND	ND	Likely pathogenic
chr1	228464876	frameshift deletion	OBSCN	p.R2206fs	ND	ND	ND	Likely pathogenic
chr1	228479642	frameshift insertion	OBSCN	p.A3461fs	ND	ND	1.00E-04	Likely pathogenic
chr1	228505223	frameshift deletion	OBSCN	p.L4541fs	ND	0.0014	0.0017	Likely pathogenic
chr1	228521482	splicing	OBSCN		ND	ND	ND	Likely pathogenic
chr1	228525846	splicing	OBSCN		ND	ND	ND	Likely pathogenic
chr1	228547775	frameshift deletion	OBSCN	p.R6395fs	ND	0.0007	3.00E-04	Likely pathogenic
chr1	228550389	frameshift deletion	OBSCN	p.R6259fs	ND	0.0011	9.00E-04	Likely pathogenic
chr1	228552733	frameshift deletion	OBSCN	p.E6298fs	ND	ND	ND	Likely pathogenic
chr1	228553810	stopgain	OBSCN	p.Q6367X	ND	ND	ND	Pathogenic
chr1	228557782	stopgain	OBSCN	p.Q6703X	ND	ND	ND	Pathogenic
chr1	228562285	splicing	OBSCN		0.004	0.0041	0.004	Likely pathogenic

chr1	228566347	frameshift insertion	OBSCN	p.Q7920fs	ND	ND	ND	Likely pathogenic
chr4	186423612	stopgain	PDLIM3	p.K144_Y145delinsX	ND	ND	ND	Likely pathogenic
chr18	3067360	frameshift insertion	MYOM1	p.G1557fs	ND	ND	ND	Likely pathogenic
chr18	3083989	frameshift insertion	MYOM1	p.I1363fs	ND	ND	ND	Likely pathogenic
chr18	3094305	splicing	MYOM1		ND	ND	ND	Likely pathogenic
chr10	18439810	splicing	CACNB2		ND	0	0.0024	Likely pathogenic
chr6	7580603	stopgain	DSP	p.Q1394X	ND	0	0	Pathogenic
chr11	2591882	missense	KCNQ1	p.G168R	ND	ND	0	Likely pathogenic
chr11	2592602	missense	KCNQ1	p.K218E	ND	ND	ND	Likely pathogenic
chr11	2790112	missense	KCNQ1	p.R518Q	ND	0	5.80E-05	Likely pathogenic
chr12	98927148	frameshift deletion	TMPO	p.P372fs	ND	0.0001	1.00E-04	Likely pathogenic
chr12	98928032	frameshift insertion	TMPO	p.N666fs	ND	ND	5.80E-05	Likely pathogenic
chr1	236891015	stopgain	ACTN2	p.R192X	ND	ND	0	Pathogenic
chr15	85360470	frameshift insertion	ALPK3	p.A131fs	ND	0	2.00E-04	Likely pathogenic
chr15	85384051	frameshift insertion	ALPK3	p.G716fs	ND	ND	ND	Likely pathogenic
chr15	85400588	frameshift deletion	ALPK3	p.G1076fs	ND	ND	ND	Likely pathogenic
chr15	85405930	stopgain	ALPK3	p.W1600X	ND	ND	ND	Pathogenic

chr15	85405970	stopgain	ALPK3	p.R1614X	ND	ND	5.80E-05	Pathogenic
chr2	220283373	frameshift insertion	DES	p.A63fs	ND	ND	ND	Likely pathogenic
chr7	128488980	missense	FLNC	p.S1624L	ND	ND	ND	Likely pathogenic
chr7	151273498	missense	PRKAG2	p.R61Q	ND	ND	ND	Likely pathogenic
chr7	151573631	frameshift deletion	PRKAG2	p.N25fs	ND	ND	ND	Likely pathogenic
chr1	155874568	missense	RIT1	p.I28T	ND	ND	ND	Likely pathogenic
chr18	29175207	missense	TTR	p.E109K	ND	ND	ND	Likely pathogenic
chr12	22047019	frameshift deletion	ABCC9	p.H579fs	ND	ND	ND	Likely pathogenic
chr12	22069894	stopgain	ABCC9	p.E184X	ND	ND	ND	Pathogenic
chr17	78081424	missense	GAA	p.S254L	0.001	0.0029	0.0028	Likely pathogenic
chr17	78083792	missense	GAA	p.D459N	0.001	0	0	Likely pathogenic
chr17	78086773	stopgain	GAA	p.Q663X	ND	ND	ND	Pathogenic
chr17	78092467	stopgain	GAA	p.E888X	ND	0.0002	3.00E-04	Likely pathogenic
chr17	78093082	frameshift deletion	GAA	p.C938fs	ND	0.0002	2.00E-04	Likely pathogenic
chr10	88476145	frameshift deletion	LDB3	p.S322fs	ND	0	0.0017	Likely pathogenic
chr6	76599857	frameshift insertion	MYO6	p.Q914fs	ND	0.003	2.00E-04	Likely pathogenic
chr6	76599857	frameshift insertion	MYO6	p.Q914fs	ND	ND	ND	Likely pathogenic
chr6	76624712	frameshift deletion	MYO6	p.Q1258fs	ND	0.0004	7.00E-04	Likely pathogenic

chr4	186066185	frameshift insertion	SLC25A4	p.S127fs	ND	ND	ND	Likely pathogenic

Table S8. Comprehensive annotation for identified genes.

Gene Symbol	Description	Coef in model	Biological Process (GO)
LPL	lipoprotein lipase	-0.071885	GO:0055095 lipoprotein particle mediated signaling;GO:0055096 low-density lipoprotein particle mediated signaling;GO:0010886 positive regulation of cholesterol storage
OR1K1	olfactory receptor family 1 subfamily K member 1	-0.06896	GO:0050911 detection of chemical stimulus involved in sensory perception of smell;GO:0007608 sensory perception of smell;GO:0050907 detection of chemical stimulus involved in sensory perception
VIT	vitrin	-0.059757	GO:0021510 spinal cord development;GO:0010811 positive regulation of cell-substrate adhesion;GO:0010810 regulation of cell-substrate adhesion
COQ4	coenzyme Q4	-0.058998	GO:0006744 ubiquinone biosynthetic process;GO:1901663 quinone biosynthetic process;GO:0006743 ubiquinone metabolic process
MYCBPAP	MYCBP associated protein	-0.053848	GO:0007283 spermatogenesis;GO:0048232 male gamete generation;GO:0007268 chemical synaptic transmission
BCL3	BCL3 transcription coactivator	-0.050093	GO:0002268 follicular dendritic cell differentiation;GO:0002266 follicular dendritic cell activation;GO:0002315 marginal zone B cell differentiation
SFMBT1	Scm like with four mbt domains 1	-0.044474	GO:0048635 negative regulation of muscle organ development;GO:0048634 regulation of muscle organ development;GO:0007517 muscle organ development
WDR49	WD repeat domain 49	-0.043116	
SLC6A6	solute carrier family 6 member 6	-0.039379	GO:0051939 gamma-aminobutyric acid import;GO:0015734 taurine transport;GO:0015812 gamma-aminobutyric acid transport
ANKRD37	ankyrin repeat domain 37	-0.039102	
TPTE2	transmembrane phosphoinositide 3-phosphatase and tensin homolog 2	-0.037443	GO:0046856 phosphatidylinositol dephosphorylation;GO:0046839 phospholipid dephosphorylation;GO:0035335 peptidyl-tyrosine dephosphorylation
LMTK3	lemur tyrosine kinase 3	-0.037438	GO:0010923 negative regulation of phosphatase activity;GO:0035305 negative

			regulation of dephosphorylation;GO:0010921 regulation of phosphatase activity
ATP6V1H	ATPase H+ transporting V1 subunit H	-0.031513	GO:0007035 vacuolar acidification;GO:0090383 phagosome acidification;GO:0050690 regulation of defense response to virus by virus
PITRM1	pitrilysin metallopeptidase 1	-0.030559	GO:0006626 protein targeting to mitochondrion;GO:0072655 establishment of protein localization to mitochondrion;GO:0070585 protein localization to mitochondrion
NDUFS6	NADH:ubiquinone oxidoreductase subunit S6	-0.03044	GO:0006120 mitochondrial electron transport, NADH to ubiquinone;GO:0010257 NADH dehydrogenase complex assembly;GO:0032981 mitochondrial respiratory chain complex I assembly
GYPB	glycophorin B (MNS blood group)	-0.029156	GO:0050900 leukocyte migration;GO:0016477 cell migration;GO:0048870 cell motility
GMNC	geminin coiled-coil domain containing	-0.028364	GO:0008156 negative regulation of DNA replication;GO:0006270 DNA replication initiation;GO:0006275 regulation of DNA replication
PLEKHA1	pleckstrin homology domain containing A1	-0.026629	GO:0033327 Leydig cell differentiation;GO:0001553 luteinization;GO:0060325 face morphogenesis
AGAP11	ArfGAP with GTPase domain, ankyrin repeat and PH domain 11	-0.019261	GO:0043547 positive regulation of GTPase activity;GO:0043087 regulation of GTPase activity;GO:0051345 positive regulation of hydrolase activity
DUSP16	dual specificity phosphatase 16	-0.017573	GO:0045208 MAPK phosphatase export from nucleus;GO:0045209 MAPK phosphatase export from nucleus, leptomycin B sensitive;GO:0045204 MAPK export from nucleus
PCDHGA4	protocadherin gamma subfamily A, 4	-0.017049	GO:0007156 homophilic cell adhesion via plasma membrane adhesion molecules;GO:0098742 cell-cell adhesion via plasma-membrane adhesion molecules;GO:0007283 spermatogenesis
CCDC174	coiled-coil domain containing 174	-0.01697	
HTR3D	5-hydroxytryptamine receptor 3D	-0.01656	GO:0007210 serotonin receptor signaling pathway;GO:0042391 regulation of membrane potential;GO:0007268 chemical synaptic transmission

TAS2R38	taste 2 receptor member 38	-0.016447	GO:0001580 detection of chemical stimulus involved in sensory perception of bitter taste;GO:0050913 sensory perception of bitter taste;GO:0050912 detection of chemical stimulus involved in sensory perception of taste
ESR1	estrogen receptor 1	-0.016415	GO:0060523 prostate epithelial cord elongation;GO:0060750 epithelial cell proliferation involved in mammary gland duct elongation;GO:0060751 branch elongation involved in mammary gland duct branching
NCAPG	non-SMC condensin I complex subunit G	-0.015784	GO:0007076 mitotic chromosome condensation;GO:0030261 chromosome condensation;GO:0000070 mitotic sister chromatid segregation
COMMD9	COMM domain containing 9	-0.015508	GO:0042632 cholesterol homeostasis;GO:0055092 sterol homeostasis;GO:0055088 lipid homeostasis
COG4	component of oligomeric golgi complex 4	-0.014892	GO:0048213 Golgi vesicle prefusion complex stabilization;GO:0006890 retrograde vesicle-mediated transport, Golgi to ER;GO:0007030 Golgi organization
UCP3	uncoupling protein 3	-0.014734	GO:0000303 response to superoxide;GO:0000305 response to oxygen radical;GO:0009409 response to cold
CEP72	centrosomal protein 72	-0.012499	GO:0033566 gamma-tubulin complex localization;GO:1904779 regulation of protein localization to centrosome;GO:0034629 cellular protein-containing complex localization
PAFAH2	platelet activating factor acetylhydrolase 2	-0.012285	GO:0016042 lipid catabolic process;GO:0007596 blood coagulation;GO:0007599 hemostasis
MIOX	myo-inositol oxygenase	-0.0104	GO:0019310 inositol catabolic process;GO:0006020 inositol metabolic process;GO:0046174 polyol catabolic process
EQTN	equatorin	-0.010094	GO:0060478 acrosomal vesicle exocytosis;GO:0007342 fusion of sperm to egg plasma membrane involved in single fertilization;GO:0045026 plasma membrane fusion
NAGPA	N-acetylglucosamine-1-phosphodiester	-0.010009	GO:0033299 secretion of lysosomal enzymes;GO:0006622 protein targeting to

	alpha-N-acetylglucosaminidase		lysosome;GO:0006623 protein targeting to vacuole
ZNF502	zinc finger protein 502	-0.009393	GO:0044789 modulation by host of viral release from host cell;GO:0044791 positive regulation by host of viral release from host cell;GO:0044794 positive regulation by host of viral process
GJB7	gap junction protein beta 7	-0.008757	GO:0055085 transmembrane transport;GO:0007267 cell-cell signaling;GO:0006810 transport
BIN1	bridging integrator 1	-0.007942	GO:1903946 negative regulation of ventricular cardiac muscle cell action potential;GO:1902960 negative regulation of aspartic-type endopeptidase activity involved in amyloid precursor protein catabolic process;GO:0106135 negative regulation of cardiac muscle cell contraction
ZNF804A	zinc finger protein 804A	-0.006747	GO:1902952 positive regulation of dendritic spine maintenance;GO:1902950 regulation of dendritic spine maintenance;GO:0097062 dendritic spine maintenance
MREG	melanoregulin	-0.006699	GO:0072385 minus-end-directed organelle transport along microtubule;GO:0032402 melanosome transport;GO:0032401 establishment of melanosome localization
PPP1R42	protein phosphatase 1 regulatory subunit 42	-0.00661	GO:0010921 regulation of phosphatase activity;GO:0035303 regulation of dephosphorylation;GO:0016311 dephosphorylation
HARS2	histidyl-tRNA synthetase 2, mitochondrial	-0.003425	GO:0006427 histidyl-tRNA aminoacylation;GO:0006418 tRNA aminoacylation for protein translation;GO:0043039 tRNA aminoacylation
SEC13	SEC13 homolog, nuclear pore and COPII coat complex component	-0.003034	GO:0090110 cargo loading into COPII-coated vesicle;GO:1904263 positive regulation of TORC1 signaling;GO:0035459 cargo loading into vesicle
TFCP2L1	transcription factor CP2 like 1	-0.002984	GO:0007028 cytoplasm organization;GO:0002070 epithelial cell maturation;GO:0008340 determination of adult lifespan
POC5	POC5 centriolar protein	-0.001794	GO:0007049 cell cycle;GO:0009987 cellular process;GO:0008150 biological_process

ZHX1	zinc fingers and homeoboxes 1	-0.001537	GO:0000122 negative regulation of transcription by RNA polymerase II;GO:0045892 negative regulation of transcription, DNA-templated;GO:1903507 negative regulation of nucleic acid-templated transcription
ZNF564	zinc finger protein 564	-0.000037	GO:0006357 regulation of transcription by RNA polymerase II;GO:0006366 transcription by RNA polymerase II;GO:0006355 regulation of transcription, DNA-templated

Table S9. Clinical status of heart tissue from published database.

Etiology	Gender	Age	Heart Weight (g)	BMI	LVEF (%)
HCMpEF	Male	46	329	27.6	55
HCMpEF	Male	51	635	24.44	57.5
HCMpEF	Male	42	297	21.8	50
HCMpEF	Male	35	404	20.99	50
HCMrEF1	Female	65	546	27.78	20
HCMrEF2	Female	53	283	20.78	25
HCMrEF3	Male	26	402	19.11	25
HCMrEF4	Male	40	634	25	30
HCMrEF5	Male	58	548	33.56	35

Table S10. 46-gene set was enriched in LVEF-reduced HCM patients after adjusting for multiple comparisons.

		HCMrEF1			HCMrEF2			HCMrEF3			HCMrEF4			HCMrEF5		
Gene set	genes included in proteome	Hits	P-value	Adjusted P-value	Hits	P-value	Adjusted P-value	Hits	P-value	Adjusted P-value	Hits	P-value	Adjusted P-value	Hits	P-value	Adjusted P-value
46-gene set	7	7	0.013	0.031	7	0.025	0.031	7	0.019	0.031	7	0.025	0.031	5	0.382	0.382

References

[1] McKenna A, Hanna M, Banks E, Sivachenko A, Cibulskis K, Kernytsky A, Garimella K, Altshuler D, Gabriel S, Daly M*, et al.* The genome analysis toolkit: A mapreduce framework for analyzing next-generation DNA sequencing data. Genome Res, 2010, 20: 1297-1303

[2] Li H, Durbin R. Fast and accurate long-read alignment with burrows-wheeler transform. Bioinformatics, 2010, 26: 589-595

[3] Price AL, Patterson NJ, Plenge RM, Weinblatt ME, Shadick NA, Reich D. Principal components analysis corrects for stratification in genome-wide association studies. Nat Genet, 2006, 38: 904-909

[4] Wang K, Li M, Hakonarson H. Annovar: Functional annotation of genetic variants from high-throughput sequencing data. Nucleic Acids Res, 2010, 38: e164